

Structural and Corrosion Resistance Behaviour of Sn-Zn Alloys on Zn Reduction and Minor Additions of Cu, Al

Nakshdeep Singh¹, Navraj Singh² and Uma Batra^{3*}

Department of Materials and Metallurgical Engg.,
PEC University of Engineering and Technology, Chandigarh, India
E-mail: *umabatra2@yahoo.com

Abstract—Traditional Sn-Pb solders are constantly being replaced with Lead-free solders due to environment related issues. The Sn-Zn Lead-free solders are the potential substitutes for Sn-Pb solders due to their close melting temperatures. Seven compositions Sn-9Zn, Sn-6.5Zn, Sn-7.5Zn, Sn-8.6Zn-0.4Cu, Sn-8Zn-1Cu, Sn-8.6Zn-0.45Al and Sn-8Zn-1Al have been investigated. The compositions of prepared alloys were determined using X-ray fluorescence (XRF). The microstructures of the prepared alloys were observed using Optical Microscope. In order to evaluate the effect of addition of Al, and Cu and reducing Zn in Sn-Zn alloy, the melting point, spreadability and corrosion resistance were evaluated and compared. Results indicate that alloying of Al into hypoeutectic Sn-Zn resulted in slightly reduced undercooling and increased pasty range while maintaining its melting temperature close to Sn-9Zn level, whereas alloying of Cu into hypoeutectic Sn-Zn resulted significantly increase in the melting temperature. The spreadability of alloys on the Copper substrate became enhanced by the addition of Al and Cu or by reduction in Zn percentage. The results suggest that reduction of Zn percent in Sn-Zn alloy from 9 percent to 6.5 percent significantly improved corrosion resistance, but alloying Sn-Zn with Cu improve corrosion resistance only marginally. In contrast, the corrosion resistance of Sn-Zn alloy was impaired on addition of Al.

Keywords: Lead-free Solder, Sn-Zn, Sn-Zn-Cu, Sn-Zn-Al, Microstructure, Spreadability, Corrosion Resistance, Tafel Extrapolation

INTRODUCTION

The development of Lead (Pb)-free solders has become an important concern for electronics industry, due to well recognised concerns on health and environmental safety related to Pb usage [1, 2]. Thus a comprehensive research on finding the alternative to replace the conventional Lead-Tin (Pb-Sn) eutectic alloy has been the focus of attention for many researchers around the world. A large number of Sn-based Pb-free solder systems including Sn-Ag, Sn-Au, Sn-Bi, Sn-Sb, Sn-Zn, Sn-Ag-Zn, Sn-Zn-In, Sn-Bi-Ag and Sn-Ag-Cu have been studied by many researchers [3–7]. Sn-9Zn alloy, a non-toxic binary Pb-free solder with melting Temperature of 198°C, closer to the eutectic temperature of Pb-Sn solder alloy, has been identified as one of the very few suitable candidates for Pb-free solder replacement [8]. The Sn-9Zn alloy possesses many advantages like: low cost, excellent mechanical properties, abundant raw material but reliability issues related to poor oxidation resistance and poor wetting ability are of major concern which result in reduction of the reliability of solder joints [9]. According to the Sn-Zn binary phase diagram shown in Fig. 1, lowering the Zn content in this alloy near to the eutectic composition, will not cause much increase in the equilibrium liquidus temperature. For that reason, it is promising to reduce the adverse effect of Zn by lowering its concentration while largely keeping its benefits of generating a eutectic melting point [10].

The present work aims to investigate the properties of Sn-Zn alloys with three Zn concentrations i.e. 6.5 wt.% Zn, 7.5 wt.% Zn and 9 wt.% Zn. In the present work, two new (Sn-Zn-Cu and Sn-Zn-Al) Lead-free solders were also investigated and two compositions viz. Sn-8.6Zn-0.4 Cu and Sn-8Zn-1Cu and two compositions Sn-8.6Zn-0.4Al and Sn-were developed.

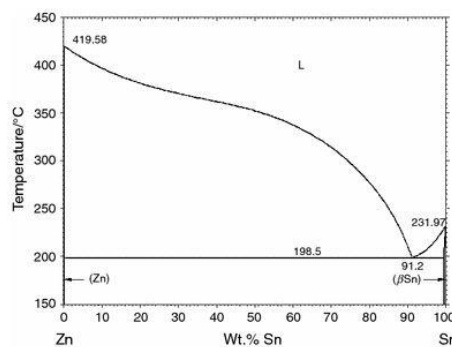


Fig. 1: Sn-Zn Equilibrium Phase Diagram

EXPERIMENTAL PROCEDURES

The Pb-free solder alloys were developed from commercially available pure Sn (99.9%) and Zn (99.9%). The starting materials were placed in a graphite crucible, heated upto 500°C for 1 hour. The Sn and Zn were covered with Lithium Chloride (LiCl) and Potassium Chloride (KCl) mixture with LiCl: KCl::1.3:1 in order to prevent their oxidation. Sn-Zn-Cu solder samples were prepared by melting pure Sn, pure Zn and Cu powder at 355°C in furnace for an hour while Sn-Zn-Al solder samples were prepared at 500°C in furnace. Stirring of the constituents was performed with an automatic stirrer fitted in the furnace, melted and then poured in a steel mould having an internal diameter of 25mm and height of 40mm to prepare the chill cast solder alloy. The alloy was homogenized at 250°C for 2 hours in muffle furnace and allowed to cool in it. The melting points of alloys were determined from their cooling curves. For this the samples were heated until they are molten and then allowed to cool slowly for crystallization. The temperature of the sample was measured as a function of time by means of a thermocouple.

The solder alloys were sectioned using metallographic sample preparation technique and polished with 0.5 μm alumina (Al_2O_3) powder. The elemental composition of solder alloys was determined using a sample with 25mm diameter and 2mm thickness using X-Ray Fluorescence Spectrometer (PW 1606). The microstructure observations were conducted on mirror polished 10x10mm samples etched with 4% HNO_3 -ethanol for about 2–3 seconds using an optical microscope with digital image acquisition. The polished samples were placed in a micro-hardness tester (LM248AT) and tested with an applied load of 25gf for 10 seconds and readings at different indentation points were noted down at room temperature to calculate the mean hardness value.

Spreadability test was conducted on 0.1 mm thick Cu sheet. The solder disc of 0.6g weight and 10mm diameter was placed on a Cu sheet and covered with an RA flux. The set-up was then put into a thermostat and held for 5 min at 250°C and then cooled in the furnace with the power off. The spreading area was measured by means of digital image analysis. The spreading ratio S is defined as $(A'-A)/A$, where A' and A represents the spreading area and the original disc area, respectively. For one solder alloy, the average spreading ratio of five tests were used to measure its wettability on Cu.

The electrochemical corrosion behaviour testing of the solder alloys was performed in 4% NaCl solution at 25°C using PGSTAT12, MetrohmAutolab, The Netherlands with analysis software (ANOVA). A three-electrode cell was used with sample as the working electrode, graphite and Ag-AgCl as the counter electrode and reference electrode, respectively. The 1 cm^2 area of alloy sample was exposed to the electrolyte. After 2 hours of immersion in NaCl solution, potentiodynamic polarization curves were obtained. The corrosion current densities and corrosion potentials of various specimens were determined from these curves by Tafel Extrapolation method. The mean value and standard deviation of the results were also calculated. The linear Tafel segments to the anodic and cathodic curves (-0.1 to +0.1 V) versus corrosion potential were extrapolated to corrosion

potential to obtain the corrosion current densities. The slopes (b_a and b_c) and the intercept correspond to corrosion current density i_{corr} . The i_{corr} (A/cm^2) was calculated using the Stan-Geary equation given.

$$i_{\text{corr}} = \frac{b_a \cdot b_c}{2.3(R_p)(b_a + b_c)}$$

Corrosion rate (C.R.) in mm/year was calculated by using following equation.

$$C.R. = 3.268 \times 10^3 \frac{i_{\text{corr}} M_w}{\rho Z}$$

Where, M_w is the molecular weight of specimen (g/mole), ρ is the density of the specimen (g/m^3) and Z is the number of electron transferred in corrosion reaction.

Figure 2 shows a flow-chart depicting the whole experimental set up.

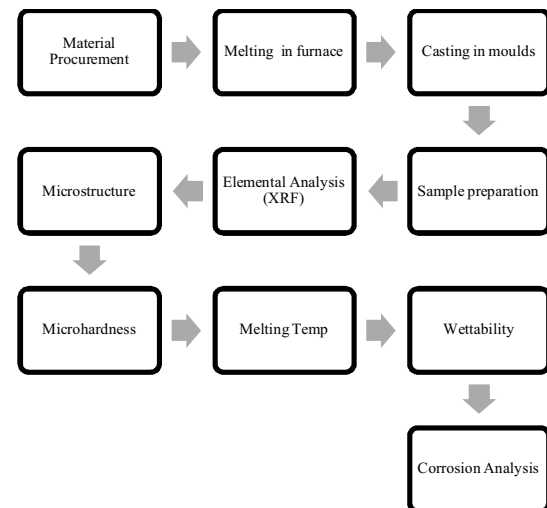


Fig. 2: Flow-Chart of the Experimental Procedures

RESULTS AND DISCUSSION

X-Ray Fluorescence

The compositions of Sn-Zn alloys, Sn-Zn-Al alloys and Sn-Zn-Cu alloys are represented in Table 1.

Table 1: XRF Results Displaying the Composition of Various Elements in the Sample

Alloy	Elemental Composition (wt %)									Theoretical Composition (wt%) Zn/Cu
	Sn	Zn	O	C	N	Cu	Na	S	Ni	
Sn-6.5Zn	77.31	6.78	6.89	5.32	1.02	0.05	0.93	0.02	0.04	6.5/0
Sn-7.5Zn	77.42	7.36	4.80	5.31	1.86	0.06	1.4	0.02	0.02	7.5/0
Sn-9Zn	72.60	8.75	6.78	8.52	2.18	0.03	2.0	0.02	0.03	9/0
Sn-8.6Zn0.4Cu	78.45	8.34	4.68	4.04	1.88	0.51	0.77	0.02	0.01	8.6/0.4
Sn-8Zn-1Cu	68.96	7.44	5.92	10.97	2.26	1.20	0.22	0.02	0.01	8/1
Sn-8.6Zn-0.4Al	88.47	8.13	0.16	1.03	0.49	0.28	0.16	0.19	0.1	8.6/0.4
Sn-8Zn-1Al	89.11	7.35	-	-	-	1.28	0.36	0.85	-	8/1

The theoretical Zn (wt.%), Cu (wt %) and Al (wt %) content of alloys was compared with experimentally determined Zn wt. % (Table 1). It is evident that there

was no burning of Zn and more than 90% of Zn added initially was recovered in every developed alloy.

MICROSTRUCTURE

The microstructure of Sn-9Zn, Sn-7.5Zn, Sn-6.5Zn, Sn-8.6Zn-0.4Cu, Sn-8Zn-1Cu, Sn-8.6Zn-0.4Al and Sn-8Zn-1Al alloys are shown in Fig. 3. Sn-9Zn alloy consists mainly of a mixture of α -Zn and β -Sn binary phases with few rods of primary Zn-phase owing to the solubility of Zn in nitric acid. On etching with the nitric acid, Zn-rich areas are seen to form dark needle like grooves. Wu, 2003 and Kim, 2003 have reported that the presence of Zn-rods in eutectic Sn-9Zn, are presumably pro-eutectic products resulting from non-equilibrium solidification in air cooling. It indicates that formation of Zn-rods in the Sn-9Zn solder joints are inevitable because the cooling rates in soldering is quite similar to air cooling. The coarser Zn rods are also considered detrimental to the mechanical reliability of the solder joint. Sn-9Zn alloy exhibited fine and closely spaced Zn-rich phase, which coarsens and become widely spaced on decrease in Zn content. Fig 3. (d) and 3. (e) represent the microstructures of Sn-8.6Zn-0.4Cu and Sn-8Zn-1Cu respectively.

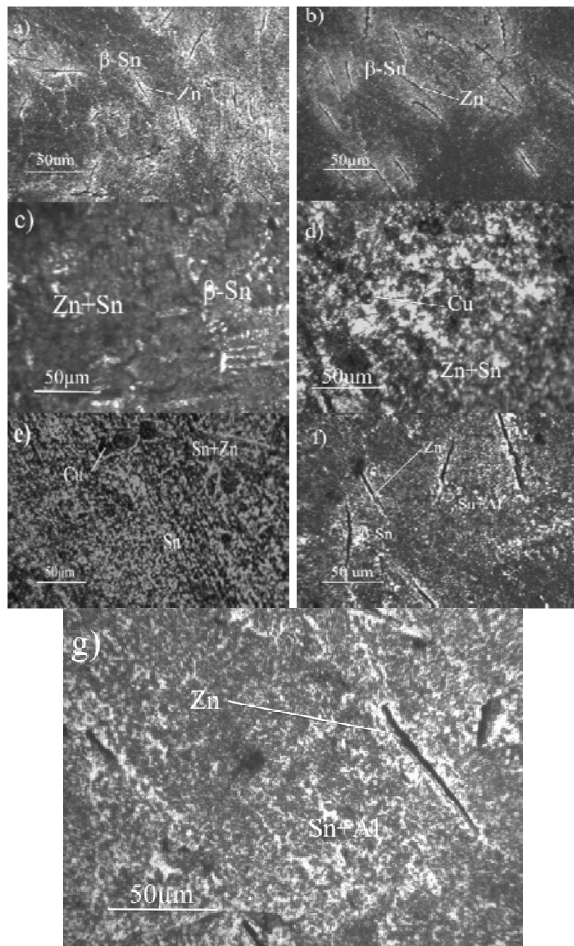


Fig. 3: Optical Images of a) Sn-6.5Zn b) Sn-7.5Zn c) Sn-9Zn d) Sn-8.6Zn-0.4Cu e) Sn-8Zn-1Cu f) Sn-8.6Zn-0.4Al g) Sn-8Zn-1Al

The former shows a bright white phase containing high concentration of Sn and the grey phase of Sn-Zn with black phase which evidently consists of Cu, while the latter shows homogeneity of microstructure relating to formation of equilibrium phases during solidification. Sn-8.6Zn-0.4Al and Sn-8Zn-1Al microstructure shows a similar image as Sn-7.5Zn.

MICROHARDNESS

Motion of dislocations, growth and configuration of the grains are the factors on which microhardness of the solder alloy depends. Therefore it depends on the microstructure, process temperature and composition. Here, microhardness of the three developed solder alloys is investigated under same ambient conditions. It was observed that with decreasing wt. % of Zn from 9 to 6.5 in Sn-Zn, the microhardness also decreased. This is attributed to the decreased fineness and increased spacing of Zn-rich phase on decrease of Zn content which can act as obstacle to the motion of dislocations on deformation. Table 2. shows the microhardness of the alloys.

Table 2: Micro-hardness of Solder Alloy

Alloy	Microhardness (HV25)
Sn-9Zn	15.8
Sn-7.5Zn	7
Sn-6.5Zn	6.4
Sn-8.6Zn-0.4Cu	17.7
Sn-8Zn-1Cu	18.6
Sn-8.6Zn-0.4Al	14.4
Sn-8Zn-1Al	14.8

Corrosion Behaviour

Figure 4 shows the experimental linear polarization curves and indicates the corrosion density (i_{corr}) for the examined Sn-9Zn, Sn-7.5Zn and Sn-6.5Zn solder alloys using both the cathodic and anodic branches of Tafel's Extrapolation. For pure Zn and Sn, value of i_{corr} for Zn is far more than that of Sn. Therefore, the addition of Zn will increase the current density. For the addition of 6.5 wt.% Zn, whereas for Sn-7.5Zn and Sn-9Zn it was respectively. A larger value of i_{corr} indicates Zn will dissolve more aggressively. Hence, an increase in Zn content leads to an increase in i_{corr} , which enhances the corrosion rate of the Sn-Zn solder. The polarisation curves indicate an increasing rate of corrosion in Sn-Zn samples with increase in Zn content. Compared with the binary compound Sn-9Zn, the two Ternary compositions (Sn-8.6Zn-0.4Cu and Sn-8Zn-1Cu) show a decreases in corrosion rates while addition of Al resulted in increase in corrosion rate (Sn-8.6Zn-0.4Al and Sn-8Zn-1Al). The corrosion potential (E_{corr}) of Sn-6.5Zn was more noble than Sn-7.5Zn and Sn-9Zn whereas E_{corr} of Sn-8Zn-1Cu was found to be more noble than Sn-8.6Zn-0.4Cu and Sn-9Zn. Table 3. is the tafel fitting parameters of all potentiodynamic polarization curves.

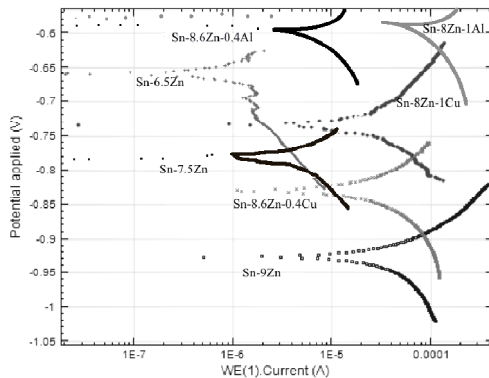


Fig. 4: Potentiodynamic Polarization Profiles of Sn-Zn Alloys and Sn-Zn-Cu Alloys in 4% NaCl Solution

At the corrosion potential, E_{corr} , rate of cathodic reduction is equal to rate of anodic reaction (metal corrosion). The polarisation curves indicate an increasing rate of corrosion in Sn-Zn samples with increase in Zn content. Compared with the binary compound Sn-9Zn, the two Ternary compositions (Sn-9Zn-0.4Cu and Sn-9Zn-1Cu) show a decrease in corrosion rates. The corrosion potential (E_{corr}) of Sn-6.5Zn was more noble than Sn-7.5Zn and Sn-9Zn whereas E_{corr} of Sn-9Zn-1Cu was found to be more noble than Sn-9Zn-0.4Cu and Sn-9Zn. Table 3. is the tafel fitting parameters of all potentiodynamic polarization curves.

Differences in the electromotive force (Δ emf) between the phases present in the alloy are generally a good indication of the corrosion potential. The standard emf of Sn and Zn are:

0.136 V, -0.763 V respectively [12]. Zn is anodic with respect to Sn, implying a galvanic driving force for the

corrosion of Zn, consequently the increase of zinc content in Sn-Zn induces a decrease of corrosion resistance. Research results reveal that the corrosion behavior of Sn-13Zn and Sn-2Zn is very similar to that of a pure Zn and Sn respectively [13]. Comparison of Corrosion rates of Sn-7Zn and Sn-9Zn have revealed that increasing Zn content in Sn-Zn alloys, induces an increase in corrosion.

Table 3. reveals that Increasing Zn content from 6.5 % to 9 % lead to increase in corrosion rate and when the content changes from Sn-9Zn to Sn-8.6Zn-0.4Cu and further to Sn-8Zn-1Cu, a decrease in corrosion rate is observed. When Effect of acid Zn, Al and Cu concentrations on corrosion rate of solder material is graphically presented for various solder. This result validates the finding obtained in OCP analysis, which states that Zn is more electrochemically active than Sn in this solution. According to Ahmad [11], Icorr is directly correlated with the dissolution process. Thus, the higher icorr value of Zn compared with that of Sn implies that the corrosion magnitude of Zn in this solution is greater than that of Sn. Potentiodynamic polarization measurement results reveal that E_{corr} did not significantly change when the Zn content was changed. However, icorr obviously increased with increasing Zn contents. The presence of the corrosion products of SnO, SnO₂, and ZnO which were determined via phase characterization after polarisation, confirmed that oxidation lead to higher corrosion rate [12].

On the other hand adding Cu to Sn-9Zn resulted in lower corrosion rates and Al resulted in higher corrosion rate. Thus it is evident that among Sn-Zn solders, Sn-6.5Zn is superior to than Sn-7.5Zn and Sn-9Zn solders. However, Sn-Zn-Cu solders have shown much more resistance to corrosion than Sn-Zn-Al solders.

Table 3: Tafel Fitting Parameters of Potentiodynamic Polarization Curves Derived from Experiment

Alloy	OCP(mV)	Ba(mV/dec)	Bc(mV/dec)	E_{corr} (mV)	J_{corr} (mA/cm ²)	Corrosion Rate (mm/ year)	Polarization Resistance (ohms)
Sn-6.5Zn	-727	16.50	14.45	-659.1	1.706E-07	0.001982	19615
Sn-7.5Zn	-783	33.5	16.6	-783.1	1.0242E-06	0.01190	4726.1
Sn-9Zn	-921	20.03	17.47	-926.9	6.0476E-06	0.07027	670.39
Sn-8.6Zn-0.4Cu	-714	15.2	19.3	-829.5	3.8485E-06	0.04471	961.15
Sn-8Zn-1Cu	-859	15.5	22.04	-733.05	3.7972E-06	0.04412	1041.10
Sn-8.6Zn-0.4Al	-760	9.67	11.63	-520	3.5466E-06	0.12087	789.8
Sn-8Zn-1Al	-810	23.72	13.43	-524	4.4546E-05	0.17022	1422.20

Melting Temperature

The solidus temperature, liquidus temperature, peak temperature and the pasty range (liquidus temp.–Solidus temp.) for Sn-9Zn, Sn-7.5Zn and Sn-6.5Zn, Sn-8.6Zn-0.4Cu, Sn-8Zn-1Cu and Sn-8.6Zn-0.4Al solder alloys during heating and cooling are given in Table 4.

An upward shift of melting temperature from 199°C to 202°C with the decrease in Zn content from 9 to 6.5 % in Sn-Zn alloys agree well with the Sn-Zn phase diagram.

As expected from the phase diagram, lowering Zn content in the eutectic Sn-9Zn alloy will not affect its equilibrium liquidus temperature (199°C). The melting temperature of hypoeutectic Sn-7.5Zn and Sn-6.5Zn were found to be 201°C and 202°C, respectively indicating that the composition obtained was a near eutectic composition, whereas melting temperature of Sn-8.6Zn-0.4Cu and Sn-8Zn-1Cu was found to be 224°C and 227°C. The Al addition increased the melting temperature to 202°C and 204°C. The pasty range of solders lies in the range of 1-

6°C which is lower than 11.5°C for Sn-Pb eutectic. On comparing the pasty range of the solders, it is found that it increases in the order Sn-9Zn > Sn-7.5Zn > Sn-6.5Zn > Sn-8Zn-1Al > Sn-8.6Zn-0.4Al > Sn-8.6Zn-0.4Cu > Sn-8Zn-1Cu.

Table 4: Comparison of Solidus Temperature (T_{start}), Liquidus Temperature (T_{end}), Peak Temperature and the Pasty Range of Solder Alloys during Heating Curve

Alloy	T _s (°C)	T _e (°C)	Pasty Range (T _e -T _s) °C	Peak Temp. (°C)
Sn-9Zn	198	199	1	199
Sn-7.5Zn	198	201	3	201
Sn-6.5Zn	198	202	4	202
Sn-8.6Zn-0.4Cu	220	226	6	226
Sn-8Zn-1Cu	222	226	4	226
Sn-8.6Zn-0.4Al	203	204	1	204
Sn-8Zn-1Al	201	202	1	202

Spreadability

With increasing Zn content the spread area is found to decrease. Zn have two opposite functions to the spread area between Sn-Zn and Cu. Below 8.9 wt.% Zn in Sn-Zn, increase in the Zn decreases the melt temperature of the solder and increase the degree of overheat, which favours the spreading. The spread area increases with the increase of Cu content from 0.4wt%, reaching the area 80.67 mm² at 0.4wt%. Thereafter, the spread area decreases with the increase of Cu content, reaching minimum area 76.70 mm² at 1.0wt%. An increase in spread area was observed in case of Sn-8.6Zn-0.4Al and Sn-8Zn-1Al. However, Zn impedes the spreading because of its oxidation and high surface tension. The two functions compete with each other and result in an optimum Zn content for wetting. Fig. 5 shows spread area increases in the order Sn-9Zn < Sn-8.6Zn-0.4Cu < Sn-8.6Zn-0.4Al < Sn-8Zn-1Cu < Sn-7.5Zn < Sn-6.5Zn.

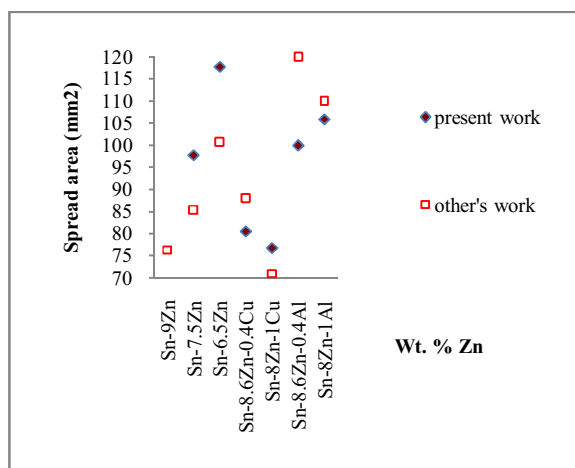


Fig. 5: Comparison of Spread Area of Present Work with Others Work

CONCLUSION

In this paper, we studied the effects of reducing the amount of Zn phase and addition of Cu and Al to the eutectic alloy i.e Sn-9Zn and corresponding changes on the microstructure, melting point, microhardness, spreadability and corrosion behaviour of Sn-Zn solder alloy. Following conclusions can be made from the results:

1. The as-cast microstructures of Sn-Zn solder is characterized by gray β Sn and dark needle-like Zn-rich phase. Large needle-like Zn rich phase is irregularly distributed.
2. Reducing the amount of Zn and Adding Al didn't significantly change the melting point (T_m) of the solder alloy. However, Adding Cu to the Sn-9Zn solder alloy resulted in higher melting point.
3. Reduced Zn content in Sn-Zn resulted in decreased microhardness because in Sn-9Zn the dislocations are not free to move due to the closely spaced Zn rich phase. Although, adding Al resulted in slight increase whereas Cu addition showed a considerable increase in value of micro-hardness.
4. Sn-6.5Zn shows the highest spread area among the all the solder alloys developed. Cu and Al additions resulted in increase in wettability of Sn-9Zn solder alloy.
5. Among the solders studied, Sn-9Zn showed higher corrosion rate than Sn-6.5Zn and Sn-7.5 Zn. The addition of Cu in Sn-9Zn resulted in decrease of corrosion rate, thus exhibiting a more noble behavior whereas adding Al resulted in high corrosion rate. The corrosion current density is quite high for Sn-9Zn solder in NaCl environment. It is also strong function of concentration of NaCl.

REFERENCES

- [1] Shen J, Gao H X, Liu Y C.(2004), Electronics Manufacturing Engineering, 5(4), pp. 150-153.
- [2] Yi Li, Kyoung-sik Moon C. P. Wong (2005). Electronics Without Lead. SCIENCE, 308(3), pp. 1419-1420.
- [3] Sabbar A, Hajjaji S E, Ben B A. (2001). Materials and Corrosion, (52), pp. 298-301.
- [4] Masayuki K j. Tadaaki S.(2005), Microelectronics Reliability, (45), pp. 1208-1214.
- [5] Wang, F., O'Keefe, M., Brinkmeyer(2009), "Journal of Alloys and Compounds" 477(1-2), pp. 267-273.
- [6] Yu S P, Lin H J(2000) J Mater Sci, 11, pp. 461-471.
- [7] Suganuma K., Kim K.S.(2007), "Sn-Zn low temperature solder, Journal of Materials Science-Materials in Electronics", Vol.18, No. 1-3, pp. 121-127.

- [8] Yamaguchi M, Ichitsubo T, Matsubara E, Kimura H, Sasamori K, Irie H, Kumamoto S, Anada T(2006), "Atomizing effect on Sn-Zn based solder alloy". *Journal of the Japan Institute of Metals*, Vol. 70, No. 2, pp. 162-165.
- [9] Wei X.Q., Huang H.Z., Zhou L., Zhang M., Liu X.D.(2007). "On the advantages of using a hypoeutectic Sn-Zn as lead-free solder material." *Materials Letters*, Vol. 61, No.3, pp. 655-658.
- [10] Lee J.E., Kim K.S., Inoue M., Jiang J.X., Sugauma K.(2008), "Effects of Ag and Cu addition on microstructural properties and oxidation resistance of Sn-Zn eutectic alloy", *Journal of Alloys and Compounds*, Vol 454., No. 1-2, pp.310-320.
- [11] Z. Ahmad(2006), "Basic concepts in corrosion, in : Principles of corrosion engineering and corrosion control", Butterworth-Heinemann, Oxford, pp. 9-56.
- [12] Muhammad Firdaus Mohd. Nazeri, Ahmed Azmin Mohamad (2014), "Corrosion measurement of Sn-Zn lead-free solders in 6M KOH.